

Higher-order exceptional surface in a pseudo-Hermitian superconducting circuit

Guo-Qiang Zhang,^{1,*} Wei Feng,¹ Yu Wang,¹ and Chui-Ping Yang^{1,†}

¹*School of Physics, Hangzhou Normal University, Hangzhou, Zhejiang 311121, China*

(Dated: March 12, 2024)

In the last few years, much attention has been paid to exceptional surfaces (ESs) owing to various important physical phenomena and potential applications. However, high-order ESs in pseudo-Hermitian systems have not been reported until now. Here, we study the high-order ES in a pseudo-Hermitian superconducting (SC) circuit system. In our proposal, the SC circuit system is composed of three circularly coupled SC cavities, where the gain and loss are balanced. According to the eigenvalue properties of the pseudo-Hermitian Hamiltonian, we derive the general pseudo-Hermitian conditions for the ternary SC system. In the special pseudo-Hermitian case with parity-time symmetry, all third-order exceptional points (EP3s) of the SC system form a third-order exceptional line in the parameter space. Under the general pseudo-Hermitian conditions, more EP3s are found, and all EP3s are located on a surface, i.e., a third-order exceptional surface is constructed. Moreover, we also investigate the eigenvalues of the pseudo-Hermitian SC circuit around EP3s. Our work opens up a door for exploring high-order ESs and related applications in pseudo-Hermitian systems.

I. INTRODUCTION

Over the past decade, exceptional points (EPs) have drawn tremendous attention [1–5]. The k th-order EP (EP k ; $k \geq 2$) refers to the spectral singularity of non-Hermitian Hamiltonians, where both k eigenvalues and eigenstates coalesce [6]. Note that at the degenerate point of Hermitian Hamiltonians, the eigenvalues are degenerate while the associated eigenvectors are still orthogonal. The spectral singularity around EPs can give rise to many intriguing phenomena, such as unidirectional invisibility [7, 8], robust wireless power transfer [9, 10], asymmetric mode switching [11, 12], enhancing spontaneous emission [13], unidirectional lasing [14], exotic topological states [15, 16], sensitivity enhancement [17–21], laser mode selection [22, 23], coherent perfect absorption [24–26], electromagnetically induced transparency [27, 28], and speeding up entanglement [29].

In many works, EPs and related applications are associated with the parity-time (\mathcal{PT}) symmetry (see, e.g., Refs. [20–26]). The \mathcal{PT} -symmetric Hamiltonian, satisfying $[H, \mathcal{PT}] = 0$, is a special subset of the non-Hermitian Hamiltonian [30]. Usually, the eigenvalues of non-Hermitian Hamiltonians are complex. However, if a non-Hermitian Hamiltonian has the \mathcal{PT} symmetry, it can also possess an entirely real eigenvalue spectrum [1–3]. When varying one of system parameters, the \mathcal{PT} -symmetric system can experience a \mathcal{PT} -symmetric phase transition in the parameter space, where the critical point of phase transition corresponds to an EP. All eigenvalues of the system are real in the \mathcal{PT} -symmetric phase, while there will be complex eigenvalues in the \mathcal{PT} -symmetry-breaking phase. Since all eigenvalues are real at the EP, the EP in \mathcal{PT} -symmetric systems has shown unique merits for potential applications (see Refs. [1–3] for reviews) in, e.g., sensitivity enhancement of the detection [20, 21] and lowering the threshold power of chaos [31].

However, the \mathcal{PT} symmetry is a very strong constraint

on the system parameters, particularly for engineering high-order EPs (i.e., EP k with $k \geq 3$). Compared with EP2s, higher-order EPs can exhibit richer physical phenomena, e.g., much richer topological characteristics [32–36] and further enhancing detection sensitivity [21, 37–39]. For relaxing this strong constraint, the \mathcal{PT} symmetry can be extended to the η -pseudo-Hermitian symmetry [40–42]. The energy-spectrum properties of the pseudo-Hermitian Hamiltonian, defined by $\eta H \eta^{-1} = H^\dagger$, are the same as those of the \mathcal{PT} -symmetric Hamiltonian. Here, η is a Hermitian invertible operator. The relationship among non-Hermitian, pseudo-Hermitian, \mathcal{PT} -symmetric and Hermitian Hamiltonians are shown in Fig. 1(a). In the pseudo-Hermitian case without \mathcal{PT} symmetry, high-order EPs and related applications have been investigated in various physical systems, including cavity-magnon systems [43–45], cavity optomechanical systems [46, 47], multicoil wireless-power-transfer systems [10], radio-frequency circuits [48], and atom-cavity QED systems [49].

Recently, the surface of EPs, i.e., exceptional surface (ES), has been introduced theoretically [50–53] and demonstrated experimentally [54, 55]. On the k th-order ES (ES k), every point is an EP k . Compared with an isolated EP, the ES has some characteristic properties. For example, the ES2 is more robust against fabrication errors and experimental uncertainties, which enable EP-based sensors to combine sensitivity and robustness [50, 55]. In addition to enhancing sensitivity with robustness [56–59], the ES2 has also been studied for controlling spontaneous emission [60], chiral light absorption [61, 62], topological behaviors [63–65], chaotic dynamics [66], and optical amplifiers [67]. Furthermore, higher-order ESs (i.e., ES k with $k \geq 3$) were theoretically proposed [68, 69] and experimentally implemented [70]. However, these works related to high-order ESs are restricted to passive non-Hermitian systems [68–70]. Up to now, there is no study on high-order ESs in pseudo-Hermitian systems with balanced gain and loss.

On the other hand, superconducting (SC) circuits are a promising platform for implementing quantum information processing and exploring various exotic phenomena (see Refs. [71–73] for reviews). In particular, Quijandría *et al.*

* zhangguoqiang@hznu.edu.cn

† yangcp@hznu.edu.cn

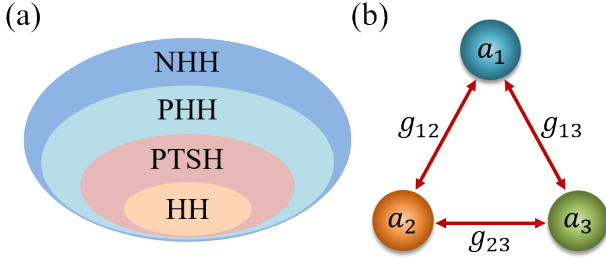


FIG. 1. (a) The relationship among non-Hermitian, pseudo-Hermitian, \mathcal{PT} -symmetric and Hermitian Hamiltonians. In the figure, the non-Hermitian Hamiltonian, pseudo-Hermitian Hamiltonian, \mathcal{PT} -symmetric Hamiltonian and Hermitian Hamiltonian are denoted as NHH, PHH, PTSH and HH, respectively. (b) Schematic diagram of the proposed SC circuit consisting of three circularly coupled SC cavities, with annihilation operators a_1 , a_2 and a_3 , respectively.

proposed the \mathcal{PT} -symmetric phase transition at the EP2 in SC circuits [74], and Dogra *et al.* simulated this on the IBM SC quantum processor [75]. In experiments, the EP2 has been observed in a dissipative SC qubit [76–79] or dissipative coupled system of two SC resonators [80]. Moreover, Han *et al.* experimentally characterize the exceptional entanglement transition around EP2 [81] and the topological invariant for EP3 [82] by measuring the dynamical evolutions of SC circuits. However, the ES in SC circuits has not been reported until now.

In this work, we theoretically investigate the high-order ES in a SC circuit, which consists of three circularly coupled SC cavities [see Fig. 1(b)]. When the system parameters satisfy certain constraints, the Hamiltonian of the system possesses the pseudo-Hermiticity. In the \mathcal{PT} -symmetric case, all EP3s of the Hamiltonian form a line in the parameter space, i.e., third-order exceptional line (EL3). When the \mathcal{PT} symmetry is extended to the η -pseudo-Hermitian symmetry, the EL3 becomes an ES3 in the parameter space. Moreover, we also study the energy spectrum of the pseudo-Hermitian SC system around EP3s. Our paper paves the way to explore ESs and related applications in SC circuits [50, 55–67]. As far as we know, it is also the first work on high-order ESs in pseudo-Hermitian systems.

This paper is organized as follows. In Sec. II, we introduce the proposed SC circuit and derive the pseudo-Hermitian conditions for the SC system. In Sec. III, we investigate the EL3 of the SC circuit in the \mathcal{PT} -symmetric case. In Sec. IV, the ES3 of the SC circuit is constructed under the pseudo-Hermitian conditions. Finally, discussions and conclusions are drawn in Sec. V.

II. MODEL

The considered SC circuit depicted in Fig. 1(b) consists of three circularly coupled SC cavities (labeled as cavity 1, cavity 2 and cavity 3, respectively). When including the losses (or gains) of three SC cavities, the non-Hermitian Hamiltonian of

the ternary SC system reads (hereafter assuming $\hbar = 1$)

$$\mathcal{H} = \sum_{n=1}^3 (\omega_n - i\kappa_n) a_n^\dagger a_n + \sum_{n,m>n} g_{nm} (a_n^\dagger a_m + a_n a_m^\dagger), \quad (1)$$

where a_n and a_n^\dagger ($n = 1, 2, 3$) are the annihilation and creation operators of cavity n with angular frequency ω_n and loss rate (or gain rate) κ_n , and g_{nm} ($m = 2, 3$) is the coupling strength between cavity n and cavity m . If cavity n is passive (active), the loss rate (gain rate) is positive (negative), i.e., $\kappa_n > 0$ ($\kappa_n < 0$). Without loss of generality, we assume that the coupling strength g_{nm} is non-negative and cavity 2 is lossy, i.e.,

$$g_{nm} \geq 0, \quad \kappa_2 > 0. \quad (2)$$

In the absence of cavity 3 (i.e., $g_{13} = g_{23} = 0$), the binary system of cavities 1 and 2 has the \mathcal{PT} symmetry when the system parameters satisfy $\omega_1 = \omega_2$ and $\kappa_1 = -\kappa_2$. This special case has been investigated in Ref. [74], where the \mathcal{PT} -symmetric phase transition at the EP2 was studied.

In this work, we study the ES3 of the ternary SC system under the pseudo-Hermitian conditions. For the convenience of following calculations, we give the corresponding matrix form H of the non-Hermitian Hamiltonian \mathcal{H} in Eq. (1) via the relation $\mathcal{H} = \alpha^\dagger H \alpha$, with $\alpha = (a_1, a_2, a_3)^T$ and

$$H = \begin{pmatrix} \omega_1 - i\kappa_1 & g_{12} & g_{13} \\ g_{12} & \omega_2 - i\kappa_2 & g_{23} \\ g_{13} & g_{23} & \omega_3 - i\kappa_3 \end{pmatrix}. \quad (3)$$

If the SC system possesses the pseudo-Hermiticity, the non-Hermitian Hamiltonian H has either (i) three real eigenvalues or (ii) one real eigenvalue and two complex-conjugate eigenvalues [40–42]. This energy-spectrum property of the pseudo-Hermitian Hamiltonian equals to that the non-Hermitian Hamiltonian H and its complex-conjugate matrix H^* have same eigenvalues [43], i.e., $|H - \lambda I| = |H^* - \lambda I| = 0$, where I is an identity matrix and λ is the eigenvalue of the Hamiltonian H . Using the relation $|H - \lambda I| = |H^* - \lambda I|$, we can obtain the pseudo-Hermitian conditions,

$$\begin{aligned} \kappa_1 + \kappa_2 + \kappa_3 &= 0, \\ \delta_1 \kappa_1 + \delta_2 \kappa_2 &= 0, \\ g_{12}^2 \kappa_3 + g_{13}^2 \kappa_2 + g_{23}^2 \kappa_1 - \delta_1 \delta_2 \kappa_3 + \kappa_1 \kappa_2 \kappa_3 &= 0, \end{aligned} \quad (4)$$

where $\delta_{1(2)} = \omega_{1(2)} - \omega_3$ is the frequency detuning of cavity 1 (cavity 2) from cavity 3. Under the pseudo-Hermitian conditions, the characteristic secular equation $|H - \lambda I| = 0$ is reduced to

$$a(\lambda - \omega_3)^3 + b(\lambda - \omega_3)^2 + c(\lambda - \omega_3) + d = 0, \quad (5)$$

where the four coefficients, a , b , c and d , are given by

$$\begin{aligned} a &= 1, \\ b &= -(\delta_1 + \delta_2), \\ c &= \delta_1 \delta_2 - (g_{12}^2 + g_{13}^2 + g_{23}^2) - (\kappa_1 \kappa_2 + \kappa_1 \kappa_3 + \kappa_2 \kappa_3), \\ d &= \delta_1 g_{23}^2 + \delta_2 g_{13}^2 - 2g_{12} g_{13} g_{23} + (\delta_1 \kappa_2 + \delta_2 \kappa_1) \kappa_3. \end{aligned} \quad (6)$$

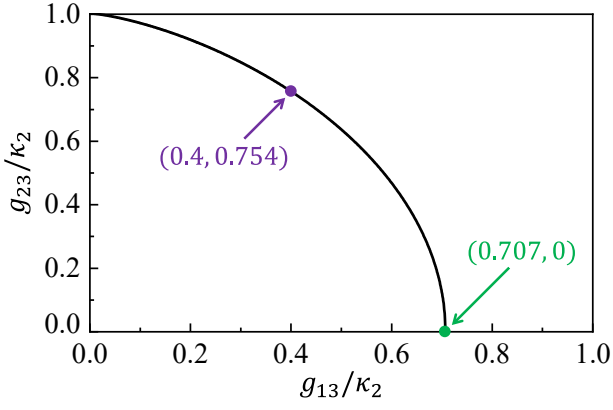


FIG. 2. The EL3 in the \mathcal{PT} -symmetric case with $\kappa_1 = 0$, obtained by numerically solving Eq. (14).

Note that Eq. (5) is a cubic equation for the eigenvalue λ , which has three roots denoted as λ_{\pm} and λ_0 . According to the root discriminant of the cubic equation with one unknown [83], the three roots λ_{\pm} and λ_0 are unequal real if the system parameters satisfy $\Delta < 0$, where

$$\Delta \equiv B^2 - 4AC \quad (7)$$

is the discriminant, with

$$A = b^2 - 3ac, \quad B = bc - 9ad, \quad C = c^2 - 3bd. \quad (8)$$

For $A = B = 0$ (satisfying $\Delta = 0$) in particular, i.e.,

$$\begin{aligned} (\kappa_1^2 + \kappa_1\kappa_2 + \kappa_2^2)(\delta_1^2 - 3\kappa_2^2) + 3\kappa_2^2(g_{12}^2 + g_{13}^2 + g_{23}^2) &= 0, \\ (\kappa_1 - \kappa_2)\kappa_1\delta_1^3 - 18\kappa_2^2g_{13}g_{23}g_{12} + \xi\delta_1\kappa_2 &= 0, \end{aligned} \quad (9)$$

λ_{\pm} and λ_0 coalesce to

$$\lambda_{\pm} = \lambda_0 = \lambda_{\text{EP3}} \equiv \omega_3 + \frac{1}{3}(\delta_1 + \delta_2), \quad (10)$$

corresponding to the EP3 of the SC system, where the coefficient ξ in Eq. (9) is given by

$$\begin{aligned} \xi &= (g_{12}^2 + 9\kappa_1\kappa_2)(\kappa_1 - \kappa_2) - g_{13}^2(8\kappa_1 + \kappa_2) \\ &\quad + g_{23}^2(\kappa_1 + 8\kappa_2) + 8(\kappa_1^3 - \kappa_2^3). \end{aligned} \quad (11)$$

In the other case of $\Delta = 0$ but $A \neq 0$ and $B \neq 0$, only λ_+ and λ_- become coalescent (i.e., $\lambda_+ = \lambda_- \neq \lambda_0$), corresponding to the EP2 of the SC system. When $\Delta > 0$, only λ_0 is still real, while λ_+ and λ_- form a complex-conjugate pair.

III. EL3 IN THE \mathcal{PT} -SYMMETRIC CASE

When cavity 1 is neutral (i.e., $\kappa_1 = 0$), the pseudo-Hermitian conditions in Eq. (4) become

$$\kappa_3 = -\kappa_2, \quad \delta_2 = 0, \quad g_{12} = g_{13}. \quad (12)$$

In this case, the non-Hermitian Hamiltonian \mathcal{H} of the system in Eq. (1) is \mathcal{PT} -symmetric, i.e., \mathcal{H} is invariant under the \mathcal{PT}

operation. This can be easily verified by simultaneously performing the \mathcal{P} operation (corresponding to $a_2 \leftrightarrow a_3$) and the \mathcal{T} operation (corresponding to $a_n \leftrightarrow -a_n$ and $i \leftrightarrow -i$) on the non-Hermitian Hamiltonian \mathcal{H} . With the \mathcal{PT} symmetry, the EP conditions given in Eq. (9) are reduced to

$$\begin{aligned} \delta_1^2 + 6g_{13}^2 + 3g_{23}^2 - 3\kappa_2^2 &= 0, \\ 9g_{23}g_{13}^2 - (4g_{23}^2 - g_{13}^2 - 4\kappa_2^2)\delta_1 &= 0. \end{aligned} \quad (13)$$

From the first equation in Eq. (13), we have $0 \leq g_{13}/\kappa_2 \leq 1/\sqrt{2}$ and $0 \leq g_{23}/\kappa_2 \leq 1$. By eliminating δ_1 in Eq. (13), we find the constraint on coupling strengths g_{13} and g_{23} given by

$$4g_{23}^2 + 2g_{13}^2 + 3\sqrt[3]{4}g_{13}^{4/3}\kappa_2^{2/3} - 4\kappa_2^2 = 0, \quad (14)$$

which describes an EL3, as plotted in Fig. 2. In the EL3, every point corresponds to an EP3, where the \mathcal{PT} -symmetric phase transition generally occurs [1–3]. For example, at $g_{13}/\kappa_2 = 0.707$ and $g_{23} = 0$ ($g_{13}/\kappa_2 = 0.4$ and $g_{23}/\kappa_2 = 0.754$) indicated by the green dot (purple dot) in Fig. 2, the corresponding three eigenvalues of the system coalesce to $\lambda_{\pm} = \lambda_0 = \lambda_{\text{EP3}} = \omega_3$ ($\lambda_{\pm} = \lambda_0 = \lambda_{\text{EP3}} = \omega_3 - 0.1923\kappa_2$), cf. Eq. (10).

Usually, one can observe the EP by measuring the energy spectrum of the system via varying the coupling strength in the experiment, where other system parameters are fixed [1–3]. In the symmetric case of $\omega_1 = \omega_2 = \omega_3$ (i.e., the three cavities are on-resonance), the three eigenvalues λ_{\pm} and λ_0 of the system, given by

$$\lambda_{\pm} = \omega_3 \pm \sqrt{2g_{13}^2 - \kappa_2^2}, \quad \lambda_0 = \omega_3, \quad (15)$$

can be obtained by solving the characteristic equation in Eq. (5) under the \mathcal{PT} -symmetric conditions given in Eq. (12). From Eq. (15), the system has three real eigenvalues (one real eigenvalue and two complex-conjugate eigenvalues) in the region $g_{13}/\kappa_2 > 1/\sqrt{2}$ ($g_{13}/\kappa_2 < 1/\sqrt{2}$). This indicates that the system is in the \mathcal{PT} -symmetric phase for $g_{13}/\kappa_2 > 1/\sqrt{2}$ and the \mathcal{PT} -symmetry-breaking phase for $g_{13}/\kappa_2 < 1/\sqrt{2}$, respectively. Particularly, the three eigenvalues coalesce to $\lambda_{\pm} = \lambda_0 = \lambda_{\text{EP3}} = \omega_3$ at $g_{13}/\kappa_2 = 1/\sqrt{2}$, corresponding to the EP3 indicated by the green dot in Fig. 2. If we vary the coupling strength g_{13} from $g_{13}/\kappa_2 > 1/\sqrt{2}$ to $g_{13}/\kappa_2 < 1/\sqrt{2}$, the system will undergo a phase transition from the \mathcal{PT} -symmetric phase to the \mathcal{PT} -symmetry-breaking phase at the EP3 with $g_{13}/\kappa_2 = 1/\sqrt{2}$. In the asymmetric case of $\omega_1 \neq \omega_2 = \omega_3$ (i.e., the three cavities are off-resonance), the EP3 still exists, but it is difficult to analytically investigate the eigenvalues of the system because the expressions of three eigenvalues are cumbersome and not shown here.

In Fig. 3, we display the energy spectrum of the Hamiltonian \mathcal{H} in Eq. (1) versus the coupling strength g_{13}/κ_2 in the \mathcal{PT} -symmetric case. Figures 3(a) and 3(b) show the real and imaginary parts of the eigenvalues λ_{\pm} and λ_0 given in Eq. (15) versus g_{13}/κ_2 in the symmetric case (i.e., $\omega_1 = \omega_2 = \omega_3$). It can be seen that the eigenvalue λ_0 is real for any values of g_{13}/κ_2 (see the solid red curves), while other two eigenvalues λ_+ and λ_- are complex (real) when

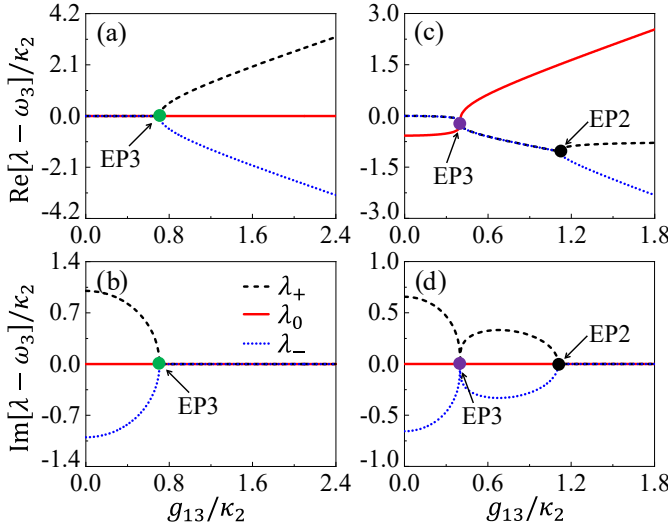


FIG. 3. The real and imaginary parts of the eigenvalue $(\lambda - \omega_3)/\kappa_2$ as a function of the coupling strength g_{13}/κ_2 in the \mathcal{PT} -symmetric case. Here $\delta_1 = g_{23} = 0$ in (a) and (b), while $\delta_1/\kappa_2 = -0.5768$ and $g_{23}/\kappa_2 = 0.7544$ in (c) and (d). Other parameters are $\kappa_1 = 0$, $\kappa_3/\kappa_2 = -1$, $\delta_2 = 0$, and $g_{12} = g_{13}$.

$g_{13}/\kappa_2 < 0.707$ ($g_{13}/\kappa_2 > 0.707$; see the dashed black and dotted blue curves). This means that in the region $g_{13}/\kappa_2 > 0.707$ ($g_{13}/\kappa_2 < 0.707$), the system is in the \mathcal{PT} -symmetric phase (\mathcal{PT} -symmetry-breaking phase). For $g_{13}/\kappa_2 = 0.707$ in particular, the three eigenvalues coalesce together (corresponding to an EP3), where the \mathcal{PT} -symmetric phase transition occurs. Compared with the symmetric case, the eigenvalues of the SC system have significantly different characteristics in the asymmetric case [i.e., $\omega_1 \neq \omega_2 = \omega_3$; cf. Figs. 3(a) and 3(c); Figs. 3(b) and 3(d)], where the results in Figs. 3(c) and 3(d) are obtained by numerically solving the characteristic equation in Eq. (5) under the \mathcal{PT} -symmetric conditions given in Eq. (12). As shown in Figs. 3(c) and 3(d), the SC system can exhibit a \mathcal{PT} -symmetric phase transition at the EP2 [rather than the EP3 in the symmetric case; cf. Figs. 3(a) and 3(b)] with $g_{13}/\kappa_2 = 1.109$, where only two eigenvalues λ_+ and λ_- (see the dashed black and dotted blue curves) are coalescent. In the \mathcal{PT} -symmetry-breaking phase with complex eigenvalues, there exists an EP3 at $g_{13}/\kappa_2 = 0.401$, marked by the purple dots in Figs. 3(c) and 3(d). Note that no \mathcal{PT} -symmetric phase transition occurs at this EP3.

IV. ES3 UNDER THE PSEUDO-HERMITIAN CONDITIONS

In the last section, we study the EP3 in the \mathcal{PT} -symmetric case of $\kappa_1 = 0$. Here we investigate the EP3 for $\kappa_1 > 0$. When $\kappa_1 > 0$, the ternary SC system can own the pseudo-Hermiticity without \mathcal{PT} symmetry. For any given value of $\kappa_1/\kappa_2 (> 0)$, we can obtain an EL3 by numerically solving Eq. (9) under the pseudo-Hermitian conditions in Eq. (4). In Fig. 4(a), we take $\kappa_1/\kappa_2 = 0.1, 1, 2$, and 3 as an example. At each point in the four EL3s, the corresponding three eigenvalues of the ternary

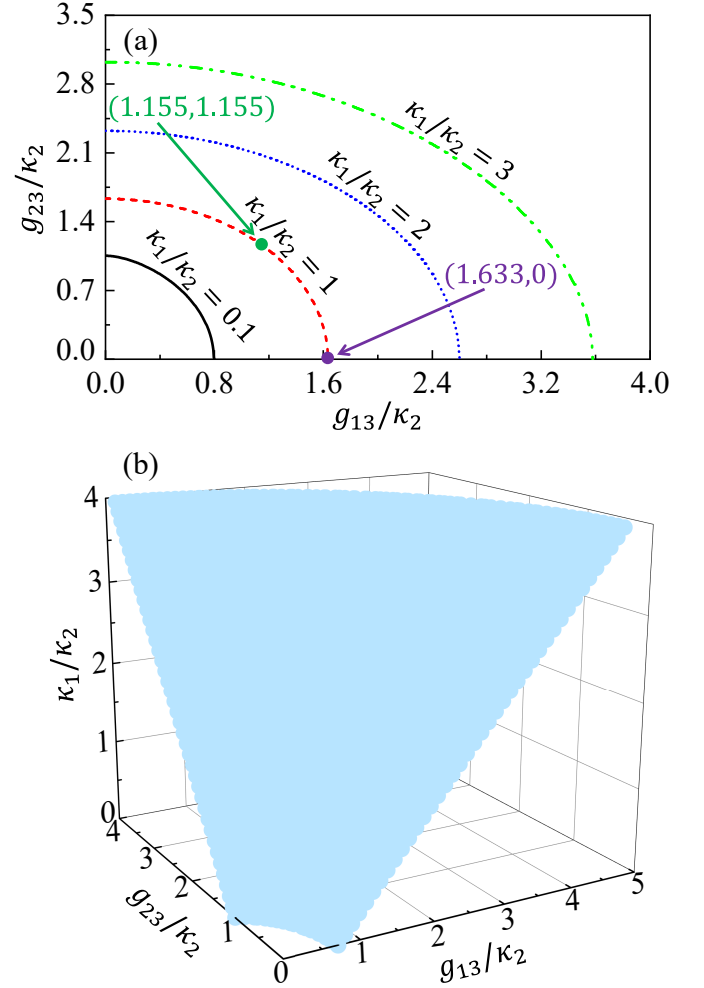


FIG. 4. (a) EL3s for different κ_1/κ_2 and (b) ES3, obtained by numerically solving Eq. (9) under the pseudo-Hermitian conditions in Eq. (4). Here $\kappa_1/\kappa_2 = 0.1$ for the (black) solid curve, $\kappa_1/\kappa_2 = 1$ for the (red) dashed curve, $\kappa_1/\kappa_2 = 2$ for the (blue) dotted curve, and $\kappa_1/\kappa_2 = 3$ for the (green) dotted-dashed curve.

SC system coalesce to one, such as $\lambda_+ = \lambda_0 = \lambda_{EP3} = \omega_3$ at $g_{13}/\kappa_2 = g_{23}/\kappa_2 = 1.155$ indicated by the green dot and $\lambda_+ = \lambda_0 = \lambda_{EP3} = \omega_3$ at $g_{13}/\kappa_2 = 1.633$ and $g_{23} = 0$ indicated by the purple dot. If we continuously vary κ_1/κ_2 , these EL3s will form a surface in the three-dimensional (3D) space $(g_{13}, g_{23}, \kappa_1)$. In Fig. 4(b), we plot the distribution of EP3s in the 3D space $(g_{13}, g_{23}, \kappa_1)$ by numerically solving Eqs. (9) and (4). These EP3s form an ES3. Note that this ES3 also contains the EL3 in the \mathcal{PT} -symmetric case with $\kappa_1 = 0$, cf. Fig. 2.

Next, we study the energy spectrum of the ternary SC system in the pseudo-Hermitian case with $\kappa_1 > 0$. For the symmetric case of $\kappa_1/\kappa_2 = 1$, $g_{12} = 0$ and $g_{23} = g_{13}$, the pseudo-Hermitian conditions in Eq. (4) are reduced to

$$\kappa_3 = -2\kappa_2, \quad \delta_1 = -\delta_2, \quad \delta_2 = \sqrt{g_{13}^2 - \kappa_2^2}. \quad (16)$$

The third equation in Eq. (16) means that there is the pseudo-Hermiticity for the system only when the coupling strength g_{13} satisfies $g_{13}^2 - \kappa_2^2 \geq 0$, i.e., $g_{13}/\kappa_2 \geq 1$. This characteristic

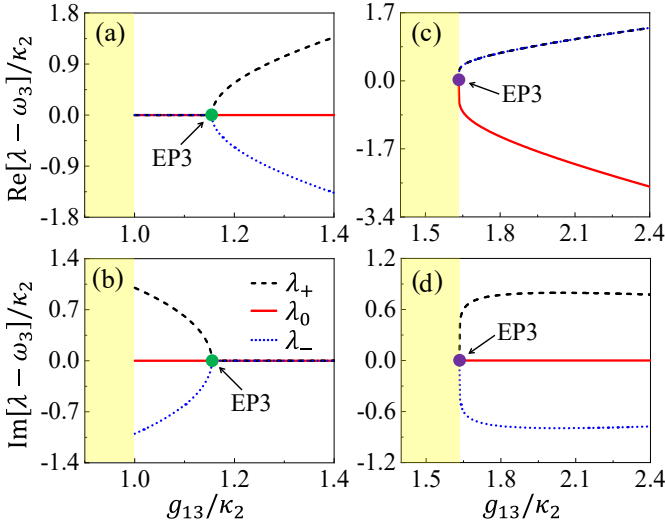


FIG. 5. The real and imaginary parts of the eigenvalue $(\lambda - \omega_3)/\kappa_2$ versus the coupling strength g_{13}/κ_2 in the pseudo-Hermitian case without \mathcal{PT} symmetry. Note that in the yellow regions, the ternary SC system does not have the pseudo-Hermiticity. Here $g_{12} = 0$, $g_{23} = g_{13}$ and $\delta_2 = \sqrt{g_{13}^2 - \kappa_2^2}$ in (a) and (b), while $g_{12} = g_{13}/\sqrt{8}$, $g_{23} = 0$ and $\delta_2 = \sqrt{3g_{13}^2/8 - \kappa_2^2}$ in (c) and (d). Other parameters are $\kappa_1/\kappa_2 = 1$, $\kappa_3/\kappa_2 = -2$ and $\delta_1 = -\delta_2$.

is significantly different from the \mathcal{PT} -symmetric case, where the ternary SC system has the \mathcal{PT} symmetry for any value of g_{13} [cf. Eq. (12) and related discussions]. Under the pseudo-Hermitian conditions in Eq. (16), the three eigenvalues of the ternary SC system are given by

$$\lambda_{\pm} = \omega_3 \pm \sqrt{3g_{13}^2 - 4\kappa_2^2}, \quad \lambda_0 = \omega_3. \quad (17)$$

In the region $g_{13}/\kappa_2 > 2/\sqrt{3}$, the ternary SC system has three real eigenvalues. For $g_{13}/\kappa_2 = 2/\sqrt{3}$ in particular, the three eigenvalues λ_{\pm} and λ_0 coalesce to $\lambda_{\pm} = \lambda_0 = \lambda_{\text{EP3}} = \omega_3$, corresponding to the EP3 indicated by the green dot in Fig. 4(a). While $1 \leq g_{13}/\kappa_2 < 2/\sqrt{3}$, λ_0 is also real but λ_{+} and λ_{-} become complex. In addition, we take an asymmetric case with $\kappa_1/\kappa_2 = 1$, $g_{12} = g_{13}/\sqrt{8}$ and $g_{23} = 0$. Now the pseudo-Hermitian conditions in Eq. (4) become

$$\kappa_3 = -2\kappa_2, \quad \delta_1 = -\delta_2, \quad \delta_2 = \sqrt{3g_{13}^2/8 - \kappa_2^2}, \quad (18)$$

which indicates that the allowed minimal value of the coupling strength g_{13} is $g_{13} = \sqrt{8/3}\kappa_2$ for ensuring $3g_{13}^2/8 - \kappa_2^2 \geq 0$. In this circumstance, we do not show the cumbersome expressions of three eigenvalues and only give the coalesced eigenvalues $\lambda_{\pm} = \lambda_0 = \lambda_{\text{EP3}} = \omega_3$ at $g_{13}/\kappa_2 = \sqrt{8/3}$, indicated by the purple dot in Fig. 4(a).

Further, we plot the energy spectrum of the pseudo-Hermitian SC system without \mathcal{PT} symmetry in Fig. 5. Note that in the yellow regions, no pseudo-Hermiticity exists. Figures 5(a) and 5(b) display the real and imaginary parts of the eigenvalues λ_{\pm} and λ_0 , given in Eq. (17), as a function of the

coupling strength g_{13}/κ_2 for the symmetric case of $\kappa_1/\kappa_2 = 1$, $g_{12} = 0$ and $g_{23} = g_{13}$. In the region $1 \leq g_{13}/\kappa_2 < 1.155$, the pseudo-Hermitian system has one real eigenvalue (see the solid red curves) and two complex-conjugate eigenvalues (see the dashed black and dotted blue curves). At the critical coupling strength $g_{13}/\kappa_2 = 1.155$, the three eigenvalues λ_{\pm} and λ_0 coalesce to $\lambda_{\pm} = \lambda_0 = \lambda_{\text{EP3}} = \omega_3$, which is an EP3 of the pseudo-Hermitian system. When $g_{13}/\kappa_2 > 1.155$, all three eigenvalues are real. In the asymmetric case of $\kappa_1/\kappa_2 = 1$, $g_{12} = g_{13}/\sqrt{8}$ and $g_{23} = 0$, the real and imaginary parts of the eigenvalues λ_{\pm} and λ_0 , obtained by numerically solving Eq. (5) under the pseudo-Hermitian conditions in Eq. (18), are also shown in Figs. 5(c) and 5(d), where the eigenvalues exist in the region $g_{13}/\kappa_2 \geq 1.633$. In addition to the EP3 at $g_{13}/\kappa_2 = 1.633$ (corresponding to $\lambda_{\pm} = \lambda_0 = \lambda_{\text{EP3}} = \omega_3$), the eigenvalue λ_0 is real (see the solid red curves) while the eigenvalues λ_{+} and λ_{-} are complex-conjugate (see the dashed black and dotted blue curves) for any allowed values of g_{13} .

V. DISCUSSIONS AND CONCLUSIONS

Before concluding, we briefly assess the experimental accessibility of the proposal in SC circuit systems. In the experiment, the typical frequency for the SC cavity can be made as 1 – 10 GHz, and the loss rate of a SC cavity is on the order of 0.1 – 1 MHz [84]. By embedding a superconducting quantum interference device (SQUID) in a SC cavity, the frequency of the SC cavity can be readily tunable via controlling the bias magnetic flux threading the SQUID loop [80]. As for the active SC cavity, its gain rate can be adjusted (ranging from 0 to 6 MHz) via controlling the drive fields on the auxiliary SC qubit, which is transversely coupled to the SC cavity [74, 85]. In addition, the tunable coupling between SC cavities (ranging from 0.62 to 16 MHz) has also been demonstrated experimentally [86]. With these accessible technologies, our proposal is experimentally accessible.

In summary, we have studied the high-order ES in a SC circuit system composed of three circularly coupled SC cavities, where the gain and loss are balanced. Using the energy-spectrum properties of the pseudo-Hermitian Hamiltonian, we derive the pseudo-Hermitian conditions for the ternary SC system. For the \mathcal{PT} -symmetric case, we find that all EP3s are located on an EL3. By tuning the coupling strength, the energy spectrum of the system displays the \mathcal{PT} -symmetric phase transition at the EP3. Under the pseudo-Hermitian conditions, all EP3s form an ES3, which contains the EL3 in the \mathcal{PT} -symmetric case. In the pseudo-Hermitian case without \mathcal{PT} symmetry, the energy spectrum of the ternary SC system around EP3s are also studied. Our work opens up a door for exploring high-order ESs in pseudo-Hermitian systems, which has potential applications in quantum technologies [50, 55–67].

ACKNOWLEDGMENTS

This work is supported by the National Natural Science Foundation of China (Grants No. U21A20436, No. 12205069 and No. 12204139).

-
- [1] L. Feng, R. El-Ganainy, and L. Ge, Non-Hermitian photonics based on parity-time symmetry, *Nat. Photonics* **11**, 752 (2017).
- [2] R. El-Ganainy, K. G. Makris, M. Khajavikhan, Z. H. Musslimani, S. Rotter, and D. N. Christodoulides, Non-Hermitian physics and \mathcal{PT} symmetry, *Nat. Phys.* **14**, 11 (2018).
- [3] Ş. K. Özdemir, S. Rotter, F. Nori, and L. Yang, Parity-time symmetry and exceptional points in photonics, *Nat. Mater.* **18**, 783 (2019).
- [4] J. Wiersig, Review of exceptional point-based sensors, *Photon. Res.* **8**, 1457 (2020).
- [5] E. J. Bergholtz, J. C. Budich, and F. K. Kunst, Exceptional topology of non-Hermitian systems, *Rev. Mod. Phys.* **93**, 015005 (2021).
- [6] W. D. Heiss, The physics of exceptional points, *J. Phys. A Math. Theor.* **45**, 444016 (2012).
- [7] Z. Lin, H. Ramezani, T. Eichelkraut, T. Kottos, H. Cao, and D. N. Christodoulides, Unidirectional Invisibility Induced by \mathcal{PT} -Symmetric Periodic Structures, *Phys. Rev. Lett.* **106**, 213901 (2011).
- [8] B. Peng, Ş. K. Özdemir, F. Lei, F. Monifi, M. Gianfreda, G. L. Long, S. Fan, F. Nori, C. M. Bender, and L. Yang, Parity-time-symmetric whispering-gallery microcavities, *Nat. Phys.* **10**, 394 (2014).
- [9] S. Assaworrorarit, X. Yu, and S. Fan, Robust wireless power transfer using a nonlinear parity-time-symmetric circuit, *Nature* **546**, 387 (2017).
- [10] X. Hao, K. Yin, J. Zou, R. Wang, Y. Huang, X. Ma, and T. Dong, Frequency-Stable Robust Wireless Power Transfer Based on High-Order Pseudo-Hermitian Physics, *Phys. Rev. Lett.* **130**, 077202 (2023).
- [11] J. Doppler, A. A. Mailybaev, J. Böhm, U. Kuhl, A. Girschik, F. Libisch, T. J. Milburn, P. Rabl, N. Moiseyev, and S. Rotter, Dynamically encircling an exceptional point for asymmetric mode switching, *Nature* **537**, 76 (2016).
- [12] H. Xu, D. Mason, L. Jiang, and J. G. E. Harris, Topological energy transfer in an optomechanical system with exceptional points, *Nature* **537**, 80 (2016).
- [13] Z. Lin, A. Pick, M. Lončar, and A. W. Rodriguez, Enhanced Spontaneous Emission at Third-Order Dirac Exceptional Points in Inverse-Designed Photonic Crystals, *Phys. Rev. Lett.* **117**, 107402 (2016).
- [14] S. Longhi and L. Feng, Unidirectional lasing in semiconductor microring lasers at an exceptional point, *Photonics Res.* **5**, B1 (2017).
- [15] H. Zhou, C. Peng, Y. Yoon, C. W. Hsu, K. A. Nelson, L. Fu, J. D. Joannopoulos, M. Soljačić, and B. Zhen, Observation of bulk Fermi arc and polarization half charge from paired exceptional points, *Science* **359**, 1009 (2018).
- [16] B. Yang, Q. Guo, B. Tremain, R. Liu, L. E. Barr, Q. Yan, W. Gao, H. Liu, Y. Xiang, J. Chen, C. Fang, A. Hibbins, L. Lu, and S. Zhang, Ideal Weyl points and helicoid surface states in artificial photonic crystal structures, *Science* **359**, 1013 (2018).
- [17] J. Wiersig, Enhancing the Sensitivity of Frequency and Energy Splitting Detection by Using Exceptional Points: Application to Microcavity Sensors for Single-Particle Detection, *Phys. Rev. Lett.* **112**, 203901 (2014).
- [18] W. Chen, Ş. K. Özdemir, G. Zhao, J. Wiersig, and L. Yang, Exceptional points enhance sensing in an optical microcavity, *Nature* **548**, 192 (2017).
- [19] G. Q. Zhang, Z. Chen, D. Xu, N. Shammah, M. Liao, T. F. Li, L. Tong, S. Y. Zhu, F. Nori, and J. Q. You, Exceptional point and cross-relaxation effect in a hybrid quantum system, *PRX Quantum* **2**, 020307 (2021).
- [20] Z. P. Liu, J. Zhang, Ş. K. Özdemir, B. Peng, H. Jing, X. Y. Lü, C. W. Li, L. Yang, F. Nori, and Y. X. Liu, Metrology with \mathcal{PT} -Symmetric Cavities: Enhanced Sensitivity near the \mathcal{PT} -Phase Transition, *Phys. Rev. Lett.* **117**, 110802 (2016).
- [21] H. Hodaei, A. U. Hassan, S. Wittek, H. Garcia-Gracia, R. El-Ganainy, D. N. Christodoulides, and M. Khajavikhan, Enhanced sensitivity at higher-order exceptional points, *Nature* **548**, 187 (2017).
- [22] L. Feng, Z. J. Wong, R. M. Ma, Y. Wang, and X. Zhang, Single-mode laser by parity-time symmetry breaking, *Science* **346**, 972 (2014).
- [23] H. Hodaei, M. A. Miri, M. Heinrich, D. N. Christodoulides, and M. Khajavikhan, Parity-time-symmetric microring lasers, *Science* **346**, 975 (2014).
- [24] Y. Sun, W. Tan, H. Li, J. Li, and H. Chen, Experimental Demonstration of a Coherent Perfect Absorber with \mathcal{PT} Phase Transition, *Phys. Rev. Lett.* **112**, 143903 (2014).
- [25] D. Zhang, X. Q. Luo, Y. P. Wang, T. F. Li, and J. Q. You, Observation of the exceptional point in cavity magnon-polaritons, *Nat. Commun.* **8**, 1368 (2017).
- [26] C. Wang, W. R. Sweeney, A. D. Stone, and L. Yang, Coherent perfect absorption at an exceptional point, *Science* **373**, 1261 (2021).
- [27] C. Wang, X. Jiang, G. Zhao, M. Zhang, C. W. Hsu, B. Peng, A. D. Stone, L. Jiang, and L. Yang, Electromagnetically induced transparency at a chiral exceptional point, *Nat. Phys.* **16**, 334 (2020).
- [28] B. Wang, Z. X. Liu, C. Kong, H. Xiong, and Y. Wu, Mechanical exceptional-point-induced transparency and slow light, *Opt. Express* **27**, 8069 (2019).
- [29] Z. Z. Li, W. Chen, M. Abbasi, K. W. Murch, and K. B. Whaley, Speeding up entanglement generation by proximity to higher-order exceptional points, *Phys. Rev. Lett.* **131**, 100202 (2023).
- [30] C. M. Bender and S. Boettcher, Real Spectra in Non-Hermitian Hamiltonians Having \mathcal{PT} Symmetry, *Phys. Rev. Lett.* **80**, 5243 (1998).
- [31] X. Y. Lü, H. Jing, J. Y. Ma, and Y. Wu, \mathcal{PT} -Symmetry-Breaking Chaos in Optomechanics, *Phys. Rev. Lett.* **114**, 253601 (2015).
- [32] K. Ding, G. Ma, M. Xiao, Z. Q. Zhang, and C. T. Chan, Emergence, Coalescence, and Topological Properties of Multiple Exceptional Points and Their Experimental Realization, *Phys. Rev. X* **6**, 021007 (2016).
- [33] I. Mandal and E. J. Bergholtz, Symmetry and higher-order exceptional points, *Phys. Rev. Lett.* **127**, 186601 (2021).

- [34] P. Delplace, T. Yoshida, and Y. Hatsugai, Symmetry-protected multifold exceptional points and their topological characterization, *Phys. Rev. Lett.* **127**, 186602 (2021).
- [35] W. Tang, X. Jiang, K. Ding, Y.-X. Xiao, Z.-Q. Zhang, C. T. Chan, and G. Ma, Exceptional nexus with a hybrid topological invariant, *Science* **370**, 1077 (2020).
- [36] Y. S. S. Patil, J. Höller, P. A. Henry, C. Guria, Y. Zhang, L. Jiang, N. Kralj, N. Read, and J. G. E. Harris, Measuring the knot of non-Hermitian degeneracies and non-commuting braids, *Nature* **607**, 271 (2022).
- [37] G. Q. Zhang, Y. P. Wang, and J. Q. You, Dispersive readout of a weakly coupled qubit via the parity-time-symmetric phase transition, *Phys. Rev. A* **99**, 052341 (2019).
- [38] C. Zeng, Y. Sun, G. Li, Y. Li, H. Jiang, Y. Yang, and H. Chen, Enhanced sensitivity at high-order exceptional points in a passive wireless sensing system, *Opt. Express* **27**, 27562 (2019).
- [39] C. Zeng, K. Zhu, Y. Sun, G. Li, Z. Guo, J. Jiang, Y. Li, H. Jiang, Y. Yang, and H. Chen, Ultra-sensitive passive wireless sensor exploiting high-order exceptional point for weakly coupling detection, *New J. Phys.* **23**, 063008 (2021).
- [40] A. Mostafazadeh, Pseudo-Hermiticity versus \mathcal{PT} -symmetry: The necessary condition for the reality of the spectrum of a non-Hermitian Hamiltonian, *J. Math. Phys.* **43**, 205 (2002).
- [41] A. Mostafazadeh, Pseudo-Hermiticity versus \mathcal{PT} -symmetry II: A complete characterization of non-Hermitian Hamiltonians with a real spectrum, *J. Math. Phys.* **43**, 2814 (2002).
- [42] A. Mostafazadeh, Pseudo-Hermiticity versus \mathcal{PT} -symmetry III: Equivalence of pseudo-Hermiticity and the presence of antilinear symmetries, *J. Math. Phys.* **43**, 3944 (2002).
- [43] G. Q. Zhang and J. Q. You, Higher-order exceptional point in a cavity magnonics system, *Phys. Rev. B* **99**, 054404 (2019).
- [44] G. Q. Zhang, Y. Wang, and W. Xiong, Detection sensitivity enhancement of magnon Kerr nonlinearity in cavity magnonics induced by coherent perfect absorption, *Phys. Rev. B* **107**, 064417 (2023).
- [45] Y. D. Hu, Y. P. Wang, R. C. Shen, Z. Q. Wang, W. J. Wu, and J. Q. You, Synthetically enhanced sensitivity using higher-order exceptional point and coherent perfect absorption, arXiv:2401.01613.
- [46] W. Xiong, Z. Li, Y. Song, J. Chen, G. Q. Zhang, and M. Wang, Higher-order exceptional point in a pseudo-Hermitian cavity optomechanical system, *Phys. Rev. A* **104**, 063508 (2021).
- [47] W. Xiong, Z. Li, G. Q. Zhang, M. Wang, H. C. Li, X. Q. Luo, and J. Chen, Higher-order exceptional point in a blue-detuned non-Hermitian cavity optomechanical system, *Phys. Rev. A* **106**, 033518 (2022).
- [48] K. Yin, X. Hao, Y. Huang, J. Zou, X. Ma, and T. Dong, High-Order Exceptional Points in Pseudo-Hermitian Radio-Frequency Circuits, *Phys. Rev. Applied* **20**, L021003 (2023).
- [49] Z. Li, X. Li, G. Zhang and X. Zhong, Realizing strong photon blockade at exceptional points in the weak coupling regime, *Front. Phys.*, **11**, 1168372 (2023).
- [50] Q. Zhong, J. Ren, M. Khajavikhan, D. N. Christodoulides, S. K. Özdemir, and R. El-Ganainy, Sensing with Exceptional Surfaces in Order to Combine Sensitivity with Robustness, *Phys. Rev. Lett.* **122**, 153902 (2019).
- [51] H. Zhou, J. Y. Lee, S. Liu, and B. Zhen, Exceptional surfaces in \mathcal{PT} -symmetric non-Hermitian photonic systems, *Optica* **6**, 190 (2019).
- [52] J. C. Budich, J. Carlstrom, F. K. Kunst, and E. J. Bergholtz, Symmetry-protected nodal phases in non-Hermitian systems, *Phys. Rev. B* **99**, 041406(R) (2019).
- [53] R. Okugawa and T. Yokoyama, Topological exceptional surfaces in non-Hermitian systems with parity-time and parity-particle-hole symmetries, *Phys. Rev. B* **99**, 041202(R) (2019).
- [54] X. Zhang, K. Ding, X. Zhou, J. Xu, and D. Jin, Experimental Observation of an Exceptional Surface in Synthetic Dimensions with Magnon Polaritons, *Phys. Rev. Lett.* **123**, 237202 (2019).
- [55] G. Q. Qin, R. R. Xie, H. Zhang, Y. Q. Hu, M. Wang, G. Q. Li, H. Xu, F. Lei, D. Ruan, and G. L. Long, Experimental Realization of Sensitivity Enhancement and Suppression with Exceptional Surfaces, *Laser Photonics Rev.* **15**, 2000569 (2021).
- [56] W. Li, Y. Zhou, P. Han, X. Chang, S. Jiang, A. Huang, H. Zhang, and Z. Xiao, Exceptional-surface-enhanced rotation sensing with robustness in a whispering-gallery-mode microresonator, *Phys. Rev. A* **104**, 033505 (2021).
- [57] M. D. Carlo, F. D. Leonardis, R. A. Soref, and V. M. Passaro, Design of an exceptional-surface-enhanced silicon-on-insulator optical accelerometer, *J. Lightwave Technol.* **39**, 5954 (2021).
- [58] M. D. Carlo, F. D. Leonardis, R. A. Soref, and V. M. Passaro, Design of a trap-assisted exceptional-surface-enhanced silicon-on-insulator particle sensor, *J. Lightwave Technol.* **40**, 6021 (2022).
- [59] S. Jiang, J. Li, Z. Li, Z. Li, W. Li, X. Huang, H. Zhang, G. Zhang, A. Huang, and Z. Xiao, Experimental realization of exceptional surfaces enhanced displacement sensing with robustness, *Appl. Phys. Lett.* **123**, 201106 (2023).
- [60] Q. Zhong, A. Hashemi, Ş. K. Özdemir, and R. El-Ganainy, Control of spontaneous emission dynamics in microcavities with chiral exceptional surfaces, *Phys. Rev. Res.* **3**, 013220 (2021).
- [61] Q. Zhong, S. Nelson, Ş. K. Özdemir, and R. El-Ganainy, Controlling direction absorption with chiral exceptional surfaces, *Opt. Lett.* **44**, 5242 (2019).
- [62] S. Soleymani, Q. Zhong, M. Mokim, S. Rotter, R. El-Ganainy, and Ş. K. Özdemir, Chiral and degenerate perfect absorption on exceptional surfaces, *Nat. Commun.* **13**, 599 (2022).
- [63] W. Tang, K. Ding, and G. Ma, Realization and topological properties of third-order exceptional lines embedded in exceptional surfaces, *Nat. Commun.* **14**, 6660 (2023).
- [64] H. Jia, R. Y. Zhang, J. Hu, Y. Xiao, S. Zhang, Y. Zhu, and C. T. Chan, Topological classification for intersection singularities of exceptional surfaces in pseudo-Hermitian systems, *Commun. Phys.* **6**, 293 (2023).
- [65] M. Stålhammar and E. J. Bergholtz, Classification of exceptional nodal topologies protected by \mathcal{PT} symmetry, *Phys. Rev. B* **104**, L201104 (2021).
- [66] L. Chen, W. Wu, F. Huang, Y. Chen, G. S. Liu, Y. Luo, and Z. Chen, Chaotic dynamics on exceptional surfaces, *Phys. Rev. A* **105**, L031501 (2022).
- [67] Q. Zhong, Ş. K. Özdemir, A. Eisfeld, A. Metelmann, and R. El-Ganainy, Exceptional Points-Based Optical Amplifiers, *Phys. Rev. Appl.* **13**, 014070 (2020).
- [68] H. Yang, X. Mao, G. Q. Qin, M. Wang, H. Zhang, D. Ruan, and G. L. Long, Scalable higher-order exceptional surface with passive resonators, *Opt. Lett.* **46**, 4025 (2021).
- [69] C. Zhang, Y. Cheng, and S. Wang, Light funneling by spin-orbit-coupled chiral particles on an arbitrary order exceptional surface, *Opt. Express* **30**, 42495 (2022).
- [70] K. Liao, Y. Zhong, Z. Du, G. Liu, C. Li, X. Wu, C. Deng, C. Lu, X. Wang, C. T. Chan, Q. Song, S. Wang, X. Liu, X. Hu, and Q. Gong, On-chip integrated exceptional surface microlaser, *Sci. Adv.* **9**, eadf3470 (2023).
- [71] Z. L. Xiang, S. Ashhab, J. Q. You, and F. Nori, Hybrid quantum circuits: Superconducting circuits interacting with other quantum systems, *Rev. Mod. Phys.* **85**, 623 (2013).
- [72] R. J. Schoelkopf and S. M. Girvin, Wiring up quantum systems, *Nature* **451**, 664 (2008).

- [73] G. Kurizki, P. Bertet, Y. Kubo, K. Mølmer, D. Petrosyan, P. Rabl, and J. Schmiedmayer, Quantum technologies with hybrid systems, *Proc. Natl. Acad. Sci. USA* **112**, 3866 (2015).
- [74] F. Quijandría, U. Naether, S. K. Özdemir, F. Nori, and D. Zueco, \mathcal{PT} -symmetric circuit QED, *Phys. Rev. A* **97**, 053846 (2018).
- [75] S. Dogra, A. A. Melnikov, and G. S. Paraoanu, Quantum simulation of parity-time symmetry breaking with a superconducting quantum processor, *Commun. Phys.* **4**, 26 (2021).
- [76] M. Naghiloo, M. Abbasi, Y. N. Joglekar, and K. W. Murch, Quantum state tomography across the exceptional point in a single dissipative qubit, *Nat. Phys.* **15**, 1232 (2019).
- [77] W. Chen, M. Abbasi, Y. N. Joglekar, and K. W. Murch, Quantum Jumps in the Non-Hermitian Dynamics of a Superconducting Qubit, *Phys. Rev. Lett.* **127**, 140504 (2021).
- [78] W. Chen, M. Abbasi, B. Ha, S. Erdamar, Y. N. Joglekar, and K. W. Murch, Decoherence-Induced Exceptional Points in a Dissipative Superconducting Qubit, *Phys. Rev. Lett.* **128**, 110402 (2022).
- [79] Z. Wang, Z. Xiang, T. Liu, X. Song, P. Song, X. Guo, L. Su, H. Zhang, Y. Du, and D. Zheng, Observation of the exceptional point in superconducting qubit with dissipation controlled by parametric modulation, *Chin. Phys. B* **30**, 100309 (2021).
- [80] M. Partanen, J. Goetz, K. Y. Tan, K. Kohvakka, V. Sevriuk, R. E. Lake, R. Kokkonen, J. Ikonen, D. Hazra, A. Mäkinen, E. Hyypä, L. Grönberg, V. Vesterinen, M. Silveri, and M. Möttönen, Exceptional points in tunable superconducting resonators, *Phys. Rev. B* **100**, 134505 (2019).
- [81] P. R. Han, F. Wu, X. J. Huang, H. Z. Wu, C. L. Zou, W. Yi, M. Zhang, H. Li, K. Xu, D. Zheng, H. Fan, J. Wen, Z. B. Yang, and S. B. Zheng, Exceptional Entanglement Phenomena: Non-Hermiticity Meeting Nonclassicality, *Phys. Rev. Lett.* **131**, 260201 (2023).
- [82] P. R. Han, W. Ning, X. J. Huang, R. H. Zheng, S. B. Yang, F. Wu, Z. B. Yang, Q. P. Su, C. P. Yang, and S. B. Zheng, Measuring topological invariants for higher-order exceptional points in quantum multipartite systems, arXiv:2402.02839.
- [83] G. A. Korn and T. M. Korn, *Mathematical Handbook for Scientists and Engineers* (McGraw-Hill, New York, 1968).
- [84] X. Gu, A. F. Kockum, A. Miranowicz, Y. X. Liu, and F. Nori, Microwave photonics with superconducting quantum circuits, *Phys. Rep.* **718-719**, 1 (2017).
- [85] G. Q. Zhang, Z. Chen, and J. Q. You, Experimentally accessible quantum phase transition in a non-Hermitian Tavis-Cummings model engineered with two drive fields, *Phys. Rev. A* **102**, 032202 (2020).
- [86] A. Baust, E. Hoffmann, M. Haeberlein, M. J. Schwarz, P. Eder, J. Goetz, F. Wulschner, E. Xie, L. Zhong, F. Quijandría, B. Peropadre, D. Zueco, J. J. G. Ripoll, E. Solano, K. Fedorov, E. P. Menzel, F. Deppe, A. Marx, and R. Gross, Tunable and switchable coupling between two superconducting resonators, *Phys. Rev. B* **91**, 014515 (2015).